Hindawi
Complexity
Volume 2022, Article ID 8344699, 11 pages
https://doi.org/10.1155/2022/8344699

Research Article

Analysis of Topological Aspects for Metal-Insulator Transition Superlattice Network

Rongbing Huang,[1] M.H. Muhammad,[2] M.K. Siddiqui,[3] S. Khalid,[3] S. Manzoor,[3] and E. Bashier[4]

[1]*School of Computer Science, Chengdu University, Chengdu, China*
[2]*College of Chemistry, School of Chemical Engineering and Energy, Zhengzhou University, Zhengzhou 450001, China*
[3]*Department of Mathematics, COMSATS University Islamabad, Lahore Campus, Pakistan*
[4]*Department of Applied Mathematics, Faculty of Mathematical Sciences, University of Khartoum, Sudan*

Correspondence should be addressed to E. Bashier; eihabbashier@gmail.com

Received 15 January 2022; Revised 17 February 2022; Accepted 28 February 2022; Published 25 March 2022

Academic Editor: Yue Song

In this research work, we have explored the physical and topological properties of the crystal structure of metal-insulator transition superlattice (GST-SL). In recent times, two-dimensional substantial have enamored comprehensive considerations owing to their novel ophthalmic and mechanical properties for anticipated employment. Recently, some researchers put their interest in modifying this material into useful forms in human life. Also, Metal-Insulator Transition Superlattice (GST–SL) is useful in form of a thin film to utilize as two-dimensional (2D) transition metal dichalcogenides (TMDs). Moreover, we have defined the computed-based bond properties such as the degree constructed topological indices and their heat of formation for single crystal and monolayered structure of Ge-Sb-Te. Also, this structure is one of the most interesting composites in modern resources of science.

1. Introduction

The germanium (Ge), Antimony (Sb), Tellurium (Te) (GST), and some other elements are present as metalloids. These metalloids lead to heat, electricity intermediates, metals, and they form large structure oxides. Metalloids are normal elements that have divided properties among metal and nonmetals, present in the Earth's outside layer [1], which occurred in an environment with a combination of organic and inorganic mixtures and other normal synthetics. The unpredictable modern abuse of these elements and possible dangers to humans are restricted in free use [2].

Some researchers put their interest in modification this material into useful forms in human life for different fields such as the GST alloy in form of a thin film is utilized as then the two-dimensional (2D) transition metal dichalcogenides (TMD) were discovered comparable applications in numerous fields [3]. These are made of cationic elements such as transition metals, group IIIA (In, Ga), and group IVA (Sn, Pb) [4]. Moreover, the anionic elements of chalcogenides (*O*, *S*, Se, Te) are essential in numerous fields. Moreover, to improve the bandgap energy of Ge–Sb–Te (GST), the physico-chemical properties are useful for sensing, in nonvolatile RAM, thermoelectric, and face change properties [5, 6]. The 2D TMDs are mainly dissimilar to pure transition bulk compounds and show new properties [7, 8]. Phase change material (PCM) properties of Ge – Sb – Te (GST) complex with a group of chalcogenides are promising technology and well known for so many years [9, 10].

A chemical graph $S = S(S_V, S_E)$ is an ordered pair of two finite sets S_V and S_E, where S_V is the set of vertices (atoms) and S_E is the set of edges (bonds) in chemical graph S [11]. The valence of molecules is usually portrayed by the vertex degrees [7, 12].

The number of edges affiliated with a vertex is identified as the degree of the vertex [13]. In this study, it is indicated by τ. Among different categories of topological indices, we will deliberate about degree-based topological indices depending on degree of end vertices of a graph, (see Table 1). For detailed study and application of these indices, see [24–27], respectively. In current circumstances, the basic aim of graph theory is the elaboration and enforcement of many contemporary scientific theories in assorted branches of chemistry. The QSPR/QSAR study is one of the essential reasons for broadening graph theory to chemistry [28].

2. Structure of GST – SL$[n]$

Another kind of PCM material named Ge – Sb – Te superlattice (GST-SL) has attracted large attention because of its ultralow power utilization. This superb exhibition has been ascribed to a special information storage system such as crystalline to crystalline stage change as compared to previous references [10, 29]. 1D semiconductor nano stares, attributable to their low dimensionality, display novel properties that discover application in numerous gadget fields [30]. The working rule of ordinary PCM gadgets depends on the changes between the metastable and amorphous crystalline stages set off either by optical. The thin film is deposited by femtosecond, picosecond, and nanosecond laser ablation [31, 32].

To this point, numerous investigations have been distributed over the most recent couple of years, proposing various distinctive atomic arrangements either for the amorphous and glasslike structure of the conceivable GST compounds or highlight by three unique stoichiometries, specifically $Ge_2Sb_2Te_5$ (most common for PMC s) [33], $Ge_1Sb_2Te_4$, and $Ge_1Sb_4Te_7$. The bulk GST intensifies two distinctive glasslike polymorphs: a metastable stage with rock salt design and a stable ground state structure at marginally low energy having a hexagonal/rhombohedral structure [34].

It is shown that the imperfection is restricted into two atomic layers of Ga, Sb, Te and shows confirmed stacking flaws. In-situ analysis demonstrated that the GeSb and Te bilayers can be effectively reconfigured into such bilayer stacking shortcomings with ensuring the arrangement of another van der Waals hole, showing a component of underlying reconfiguration of the building block in layered Ge – Sb – Te compounds [35]. The enormous distinction of dielectric capacities between the amorphous and glass-like structure of Ge – Sb – Te-based stage change materials (PCM s) utilized in-memory storage gadgets likewise influences their Schottky barrier heights (SBHs) and consequently their electric gadget properties. Here, the SBHs of each structure of $Ge_2Sb_2Te_5$, GeSb, GeSe, and SnTe are found by thickness of useful supercell computations [2].

The worldwide substance stoichiometry of the material and the local substance stoichiometry of individual layer blocks are needed to have a protecting band hole as per the electron checking model examination. The electron property can be changed by changing the local stoichiometry, for example, creating flaws around van der Waals holes (Figure 1) [10]. Moreover, the unite cell and generalized structure of GST – SL$[n]$ are depicted in Figure 2.

After some basic computation, we can see that $|V(\text{GST} - \text{SL}[n])| = 9n + 3$ and $|E(\text{GST} - \text{SL}[n])| = 13n$. The principle strategy utilized here is the way to deal with edge partitioning and vertice degree calculating (see Table 2).

2.1. Computations of Results for GST – SL$[n]$

(i) The general Randi $\acute{c}$ index of GST – SL$[n]$.

$$R_\alpha(S) = (n+2)(1\times 3)^\alpha + (2n+6)(2\times 3)^\alpha + (2n)(3\times 3) + (8n-8)(3\times 4). \tag{1}$$

For $\alpha = 1, -1, 1/2, -1/2$, we have

$$\begin{aligned} R_1(\text{GST}-\text{SL}) &= 3(43n-18),\\ R_{-1}(\text{GST}-\text{SL}) &= \frac{14n}{9}+1,\\ R_{1/2}(\text{GST}-\text{SL}) &= 6\sqrt{6}-14\sqrt{3}+(6+17\sqrt{3}+2\sqrt{6})n,\\ R_{-1/2}(\text{GST}-\text{SL}) &= \sqrt{6}-\frac{2}{\sqrt{3}}+\left(\frac{2}{3}+\frac{5}{\sqrt{3}}+\sqrt{\frac{2}{3}}\right)n. \end{aligned} \tag{2}$$

(ii) The atom bond connectivity index of GST – SL$[n]$.

The ABC index with the help of Tables 1 and 2 is

$$\begin{aligned} \text{ABC}(G) &= \sqrt{\frac{2}{3}}(n+2)++\frac{1}{\sqrt{2}}(2n+6)+\frac{2}{3}(2n)+\frac{\sqrt{5}}{2\sqrt{3}}(8n-8)\\ &= \left(\frac{4\sqrt{5}}{\sqrt{3}}+\frac{4}{3}+\sqrt{2}+\sqrt{\frac{2}{3}}\right)n+3\sqrt{2}+\frac{2\sqrt{2}}{\sqrt{3}}-\frac{4\sqrt{5}}{\sqrt{3}}. \end{aligned} \tag{3}$$

(iii) The geometric arithmetic index of GST – SL$[n]$.

The GA index with the help of Tables 1 and 2 is

Table 1: Topological descriptors.

Topological descriptors	Expression
The Randi´c index R_α with $\alpha = 1, -1, 1/2, -1/2$	$(\tau(a) \times \tau(s))^\alpha$
The atom bond connectivity index ABC(S) [14–17]	$\sqrt{\tau(a) + \tau(s) - 2/\tau(a) \times \tau(s)}$
The geometric arithmetic index GA(S) [14–17]	$2\sqrt{\tau(a) \times \tau(s)}/\tau(a) + \tau(s)$
The first Zagreb index $M_1(S)$ [14–17]	$\tau(a) + \tau(s)$
The second Zagreb index $M_2(S)$ [14, 15, 17]	$\tau(a) + \tau(s)$
The hyper Zagreb index HM(S) [18]	$[\tau(a) + \tau(s)]^2$
The forgotten index $F(S)$ [19]	$(\tau(a))^2 + (\tau(s))^2$
The augmented Zagreb index AZI(S) [20]	$(\tau(a)\tau(s)/\tau(a) + \tau(s) - 2)^3$
The Balaban index $J(S)$ [21, 22]	$(m/m - n + 2)1/\sqrt{\tau(a)\tau(s)}$
The redefined first Zagreb index $\mathrm{ReZG}_1(S)$ [23]	$\tau(a) + \tau(s)/\tau(a)\tau(s)$
The redefined second Zagreb index $\mathrm{ReZG}_2(S)$ [23]	$\tau(a)\tau(s)/\tau(a) + \tau(s)$
The redefined third Zagreb index $\mathrm{ReZG}_3(S)$ [23]	$(\tau(a)\tau(s))(\tau(a) + \tau(s))$

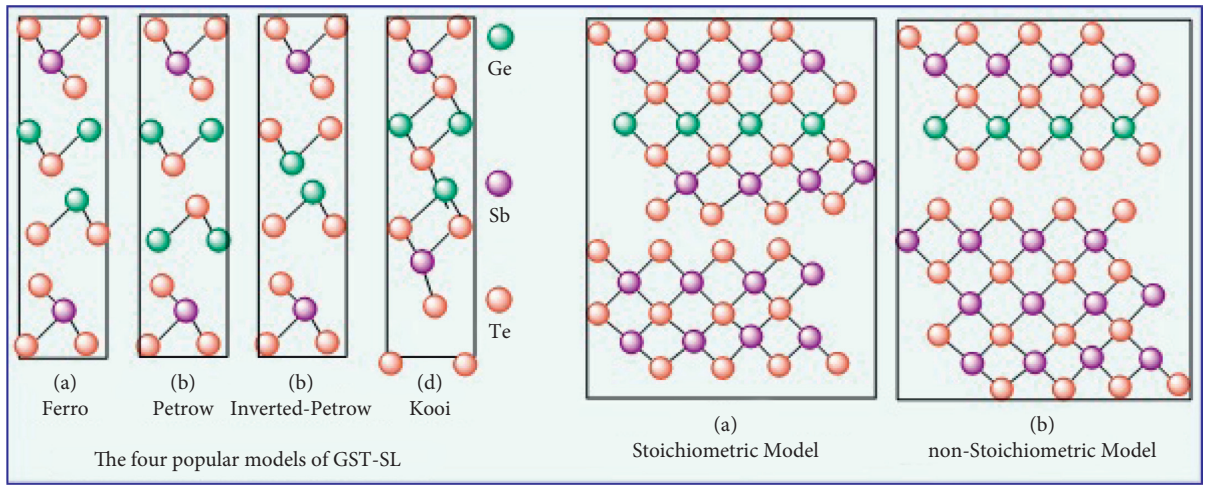

Figure 1: The general structure of (GST − SL).

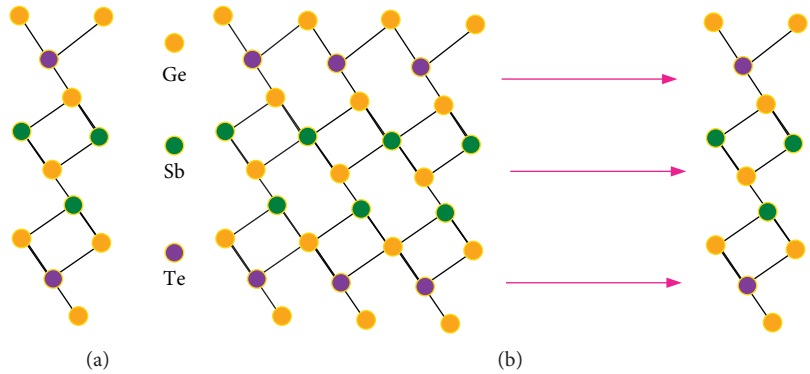

Figure 2: (a) Unit cell. (b) Generalized structure of GST − SL$[n]$.

Table 2: Edge partition of GST − SL$[n]$.

$(\tau(y), \tau(z))$	Number of repetitions	Types of edges
$(1, 3)$	$n + 2$	S_{E_1}
$(2, 3)$	$2n + 6$	S_{E_2}
$(3, 3)$	$2n$	S_{E_3}
$(3, 4)$	$8n - 8$	S_{E_4}

$$\begin{aligned}\mathrm{GA}(S) &= \frac{\sqrt{3}}{2}(n+2) + \frac{2\sqrt{6}}{5}(2n+6) + \frac{2\sqrt{9}}{6}(2n) \\ &\quad + \frac{2\sqrt{12}}{7}(8n-8) \\ &= \left(2 + \frac{4\sqrt{6}}{5} + \frac{71\sqrt{3}}{14}\right)n + \frac{12\sqrt{6}}{5} - \frac{25\sqrt{3}}{7}.\end{aligned} \tag{4}$$

(iv) The first Zagreb index of GST − SL[n].

The first Zagreb index by using Tables 1 and 2 is

$$M_1(\mathrm{GST}-SL) = 4(n+2) + 5(2n+6) + 6(2n) + 7(8n-8) = 82n - 18. \tag{5}$$

(v) The second Zagreb index of GST − SL[n].

The second Zagreb index by using Tables 1 and 2 is

$$M_2(\mathrm{GST}-SL) = 3(n+2) + 6(2n+6) + 9(2n) + 12(8n-8) = 129n - 54. \tag{6}$$

(vi) The hyper Zagreb index of GST − SL[n].

The hyper Zagreb index by using Tables 1 and 2 is

$$\mathrm{HM}(\mathrm{GST}-\mathrm{SL}) = 16(n+2) + 25(2n+6) + 36(2n) + 49(8n-8) = 530n - 210. \tag{7}$$

(vii) The forgotten index of GST − SL[n].

The forgotten index calculated by using Tables 1 and 2 is

$$F(\mathrm{GST}-\mathrm{SL}) = 10(n+2) + 13(2n+6) + 18(2n) + 25(8n-8) = 272n - 102. \tag{8}$$

(viii) The augmented Zagreb index of GST − SL[n].

The augmented Zagreb index with the help of Tables 1 and 2 is

$$\begin{aligned}\mathrm{AZI}(\mathrm{GST}-\mathrm{SL}) &= \left(\frac{3}{2}\right)^3(n+2) + 8(2n+6) + \left(\frac{9}{4}\right)^3(2n) + \left(\frac{12}{5}\right)^3(8n-8) \\ &= \frac{610993}{4000}n - \frac{27921}{500}.\end{aligned} \tag{9}$$

(xi) The Balaban index of GST − SL[n].

It is easy to see that the Balaban index by using Tables 1 and 2 is

$$\begin{aligned}J(\mathrm{GST}-\mathrm{SL}) &= \frac{13n}{13n-9n-3+2}\left[\frac{1}{\sqrt{3}}(n+2) + \frac{1}{\sqrt{6}}(2n+6) + \frac{1}{3}(2n) + \frac{1}{\sqrt{12}}(8n-8)\right] \\ &= \frac{13n}{4n-1}\left[\left(\frac{5}{\sqrt{3}} + \sqrt{\frac{2}{3}} + \frac{2}{3}\right)n - \frac{2}{\sqrt{3}} + \sqrt{6}\right].\end{aligned} \tag{10}$$

(x) The redefined first Zagreb index of GST − SL[n].

The redefined first Zagreb index with the help of Tables 1 and 2 is

$$\begin{aligned}\mathrm{ReZG}_1(\mathrm{GST}-\mathrm{SL}) &= \frac{4}{3}(n+2)+\frac{5}{6}(2n+6)+\frac{6}{9}(2n)+\frac{7}{12}(8n-8)\\ &= 3(3n+1).\end{aligned} \tag{11}$$

(xi) The redefined second Zagreb index of GST − SL[n].

The redefined second Zagreb index by using Tables 1 and 2 is

$$\begin{aligned}\mathrm{ReZG}_2(\mathrm{GST}-\mathrm{SL}) &= \frac{3}{4}(n+2)+\frac{6}{5}(2n+6)+\frac{9}{6}(2n)+\frac{12}{7}(8n-8)\\ &= \frac{2781n}{140}-\frac{351}{70}.\end{aligned} \tag{12}$$

(xii) The redefined third Zagreb index of GST − SL[n]. The Redefined third Zagreb index by using Tables 1 and 2 is:

$$\begin{aligned}\mathrm{ReZG}_3(\mathrm{GST}-\mathrm{SL}) &= 12(n+2)+30(2n+6)+54(2n)+84(8n-8)\\ &= 852n-468.\end{aligned} \tag{13}$$

3. Applications and Discussion of Computed Results

The geometric arithmetic index gives improved prediction as compared to other descriptors. We can easily see that the heat formation of GST − SL[n] is lower as the values of n increases. The first and the second Zagreb indices are established to appear within specific estimated expressions for the total π-electron energy [7, 20]. The augmented Zagreb index gives better correlation for measuring the strain energy of molecules.

The computed numerical results of Randi$\acute{c}$ indices are portrayed in Tables 3 and 4. The graphical illustration of $R_\alpha(S)$ for $\alpha = 1, -1, 1/2, -1/2$ is characterized in Figures 3 and 4.

We can use equation (14) for the transformation of Randi c indices into the approximate heat of formation for GST − SL[n].

$$\begin{aligned}H_{R_1(S)} &= 1030\cdot\left(-0.0094\cdot R_1(S)+3.0145\right),\\ H_{R_{-1}(S)} &= 1030\cdot\left(-0.6133\cdot R_{-1}(S)+4.7743\right),\\ H_{R_{1/2}(S)} &= 1030\cdot\left(-0.0810\cdot R_{1/2}(S)+3.9374\right),\\ H_{R_{-1/2}(S)} &= 1030\cdot\left(-0.2913\cdot R_{-1/2}(S)+4.1071\right).\end{aligned} \tag{14}$$

The computed numerical results of ABC index and GA index are portrayed in Table 5. The graphical illustration of these indices is characterized in Figure 5. The transformation of ABC index and GA index into the approximate heat of formation of GST − SL[n] at any level can be estimated with the help of the following equation:

$$\begin{aligned}H_{\mathrm{ABC}} &= 1040\cdot(-0.0045\cdot\mathrm{ABC}-3.4699),\\ H_{\mathrm{GA}} &= 1030\cdot(-0.0917\cdot\mathrm{GA}+2.0126).\end{aligned} \tag{15}$$

The computed numerical results for the first and the second Zagreb indices are shown in Table 6, while their graphical illustration is shown in Figure 6. The transformation of the first and the second Zagreb indices into the approximate heat of formation of GST − SL[n] at any level can be exercised with the help of the equation as follows:

$$\begin{aligned}H_{M_1} &= 1030\cdot\left(-0.045\cdot M_1+4.3142\right),\\ H_{M_2} &= 1030\cdot\left(-0.0094\cdot M_2+3.0145\right).\end{aligned} \tag{16}$$

Numerical comparison of hyper Zagreb index and forgotten index is shown in Table 7, while graphically, their comparison is shown in Figure 7 Equation (17) can be employed for the transformation of hyper and forgotten indices into the approximate heat of formation of GST − SL[n] at any cubic level.

$$\begin{aligned}H_{\mathrm{HM}}(S) &= 1020\cdot(-0.0238\cdot\mathrm{HM}(S)+3.4663),\\ H_F(S) &= 1030\cdot(-0.008\cdot F(S)+3.6558).\end{aligned} \tag{17}$$

Table 3: Comparison of R_1 and R_{-1} with their respective heat of formation for GST – SL[n].

[n]	R_1	H_{R_1}	R_{-1}	$H_{R_{-1}}$
[21]	75	2378.785	2.555 6	3303.159 0
[22]	204	1129.807	4.111 1	2320.551 2
[14]	333	−119.171	5.666 7	1337.943 4
[3]	462	−1368.149	7.222 2	355.272 5
[9]	591	−2617.127	8.777 8	−627.3985
[12]	720	−3866.105	10.333 3	−1610.0063
[31]	849	−5115.083	11.888 9	−2592.6709

Table 4: Comparison of $R_{1/2}$ and $R_{-1/2}$ with their respective heat formation for GST – SL[n].

[n]	$R_{1/2}$	$H_{R_{1/2}}$	$R_{-1/2}$	$H_{R_{-1/2}}$
[21]	30.792 1	2755.171 6	5.664 7	2530.682 1
[22]	71.135 9	1051.452 9	10.034 6	1219.541 7
[14]	111.479 8	−652.2699	14.404 5	−91.5988
[3]	151.823 6	−2355.9886	18.774 4	−1402.7392
[9]	192.167 4	−4059.7073	23.144 3	−2713.8796
[12]	232.511 2	−5763.4260	27.514 3	−4025.0501
[31]	272.855 1	−7467.1489	31.884 2	−5336.1905

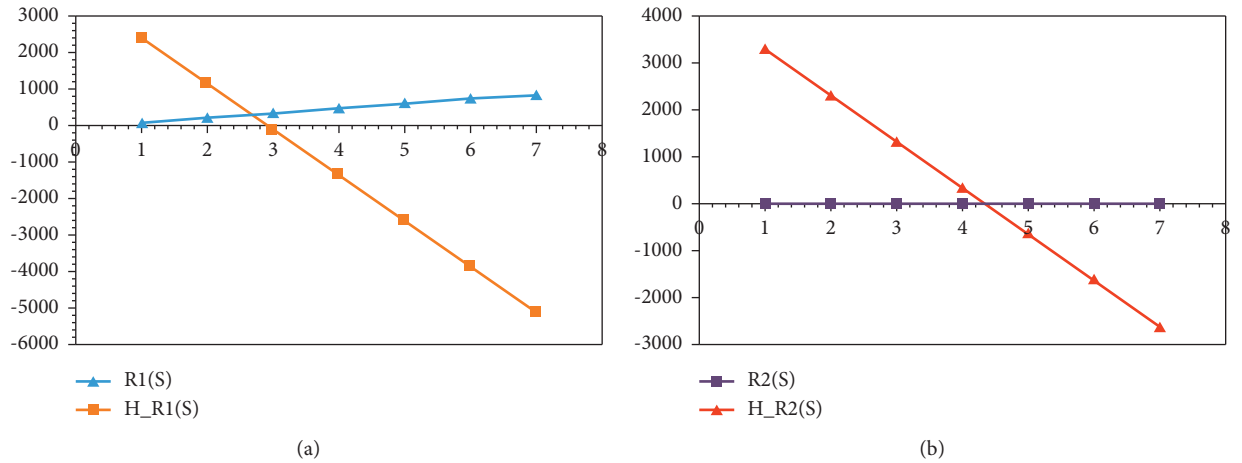

Figure 3: (a) Comparison of Randi c index for $\alpha = 1$ with heat of formation. (b) Comparison of Randi c index for $\alpha = -1$ with heat of formation.

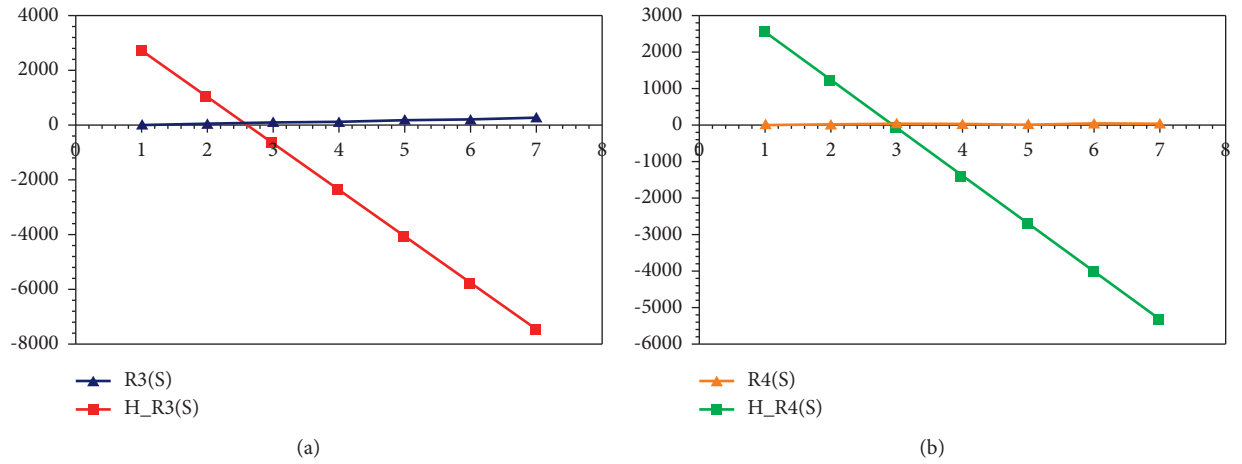

Figure 4: (a) Randi c index for $\alpha = 1/2$ with heat of formation, (b) Randi c index for $\alpha = -1/2$ with heat of formation.

Table 5: Comparison of ABC index and GA index with their respective heat of formation for GST – SL[n].

[n]	ABC	H_{ABC}	GA	H_{GA}
[21]	9.439 7	−3652.8738	12.436 4	898.3476
[22]	18.167 7	−3693.7208	25.18	−305.2982
[14]	26.895 7	−3734.569	37.923 6	−1508.9439
[3]	35.623 7	−3775.4149	50.667 1	−2712.5803
[9]	44.351 8	−3816.2624	63.410 7	−3916.2260
[12]	53.079 8	−3857.1095	76.154 3	−5119.8718
[31]	61.807 8	−3897.9565	88.897 8	−6323.5081

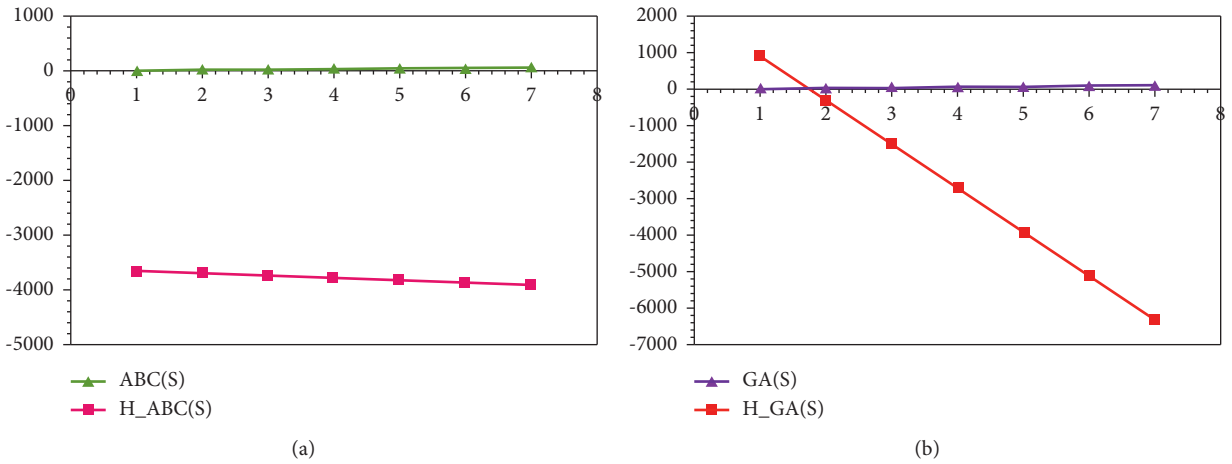

Figure 5: (a) The ABC index with heat of formation (b) The GA index with heat of formation.

Table 6: Comparison of Zagreb indices with their respective heat of formations for GST – SL[n].

[n]	M_1	H_{M_1}	M_2	H_{M_2}
[21]	64	2424.826 0	75	2378.785
[22]	146	1157.926 0	204	1129.807 0
[14]	228	−108.9740	333	−119.1710
[3]	310	−1375.8740	462	−1368.1490
[9]	392	−2642.7740	591	−2617.1270
[12]	474	−3909.6740	720	−3866.1050
[31]	556	−5176.5740	849	−5115.0830

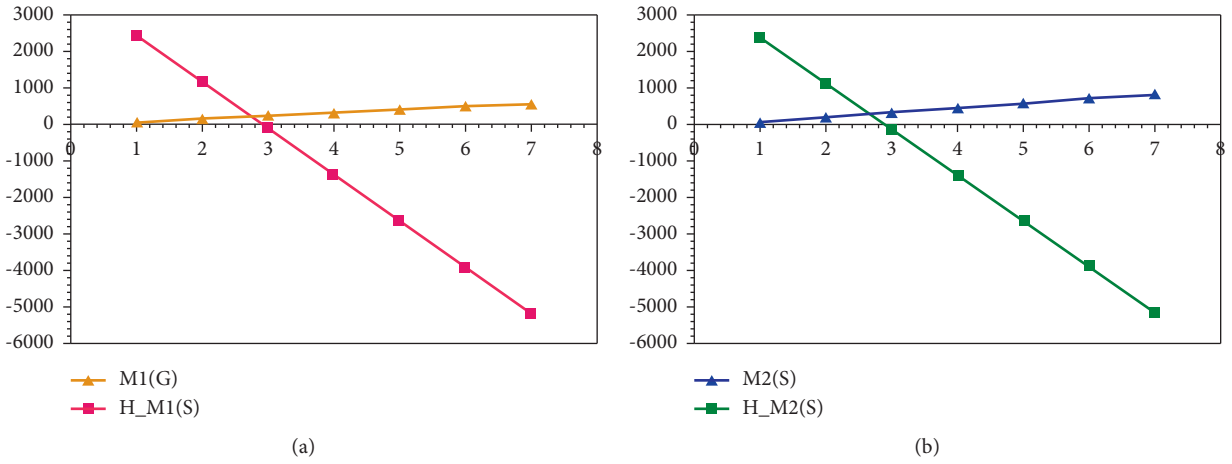

Figure 6: (a) The rirst Zagreb index with heat of formation. (b) The second Zagreb index with heat of formation.

Table 7: Comparison of HM and F indices with their respective heat of formation for GST – SL[n].

[n]	HM	H_{HM}	F	H_F
[21]	320	−5252.6940	170	2364.6740
[22]	850	−18118.9740	442	123.3940
[14]	1380	−30985.2540	714	−2117.8860
[3]	1910	−43851.5340	986	−4359.1660
[9]	2440	−56717.8140	1258	−6600.4460
[12]	2970	−69584.0940	1530	−8841.7260
[31]	3500	−82450.3740	1802	−11083.006

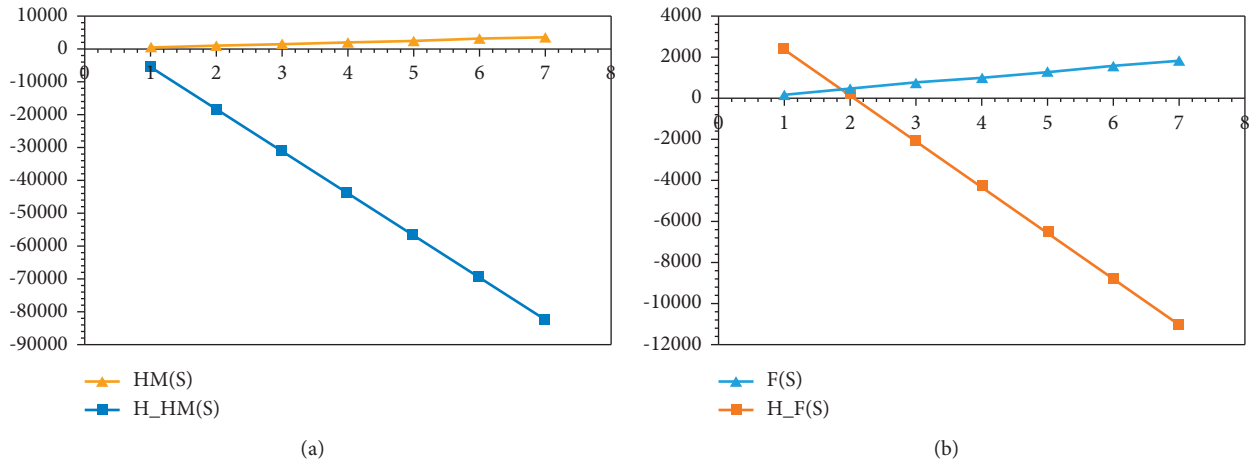

Figure 7: (a) The hyper Zagreb index with heat of formation. (b) The forgotten index with heat of formation.

Table 8: Comparison of AZI and J indices with their respective heat of formation for GST – SL[n].

[n]	AZI	H_{AZI}	J	H_J
[21]	96.906 3	1711.769 2	24.547	−6023.6551
[22]	249.654 5	−490.8599	37.271 4	−8256.9399
[14]	402.402 8	−2693.4904	51.070 6	−10678.8652
[3]	555.151	−4896.1194	65.084 8	−13138.5254
[9]	707.899 3	−7098.7499	79.178 1	−15612.0687
[12]	860.647 5	−9301.3790	93.309 3	1486.552 8
[31]	1013.396	−11504.0123	107.461 5	361.706 6

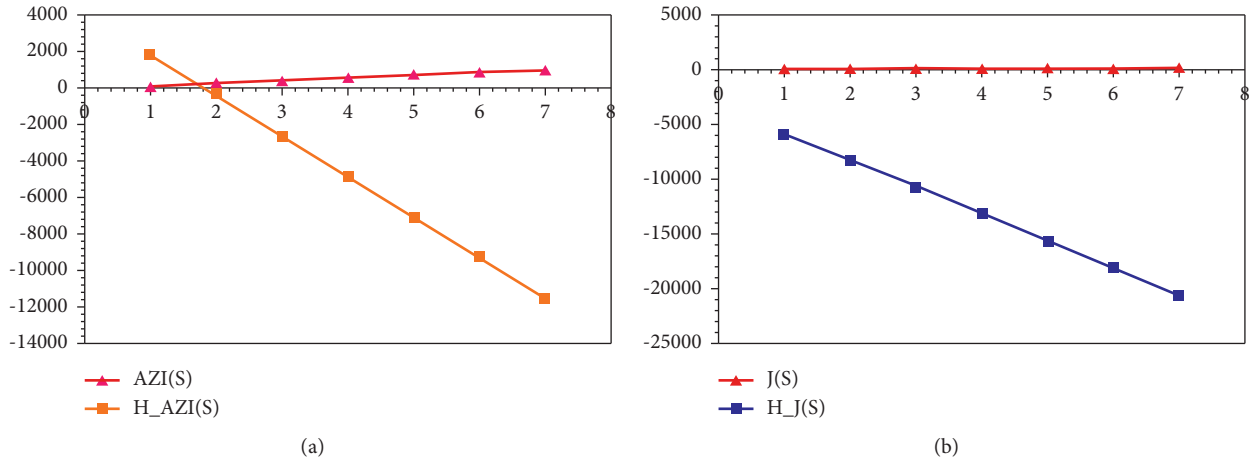

Figure 8: (a) The augmented Zagreb index with heat of formation. (b) The Balaban index with heat of formation.

Table 9: Comparison of the redefined Zagreb rntropies with their respective heat of formations for GST − SL[n].

[n]	$ReZG_1$	H_{ReZG_2}	$ReZG_2$	H_{ReZG_2}	$ReZG_3$	H_{ReZG_3}
[21]	2	2371.060	14.85	172.782 5	384	1548.090
[22]	21	−5691.780	34.714 3	−2793.9507	1236	−2839.710
[14]	30	−9511.020	54.578 6	−5760.6839	2088	−7227.51
[3]	39	−13330.260	74.442 9	−8727.4171	2940	−11615.31
[9]	48	−17149.5	94.307 1	−11694.1354	3792	−16003.11
[12]	57	−20968.74	114.171 4	−14660.8686	4644	−20390.91
[31]	66	−24787.98	134.035 7	−17627.6018	5496	−24778.71

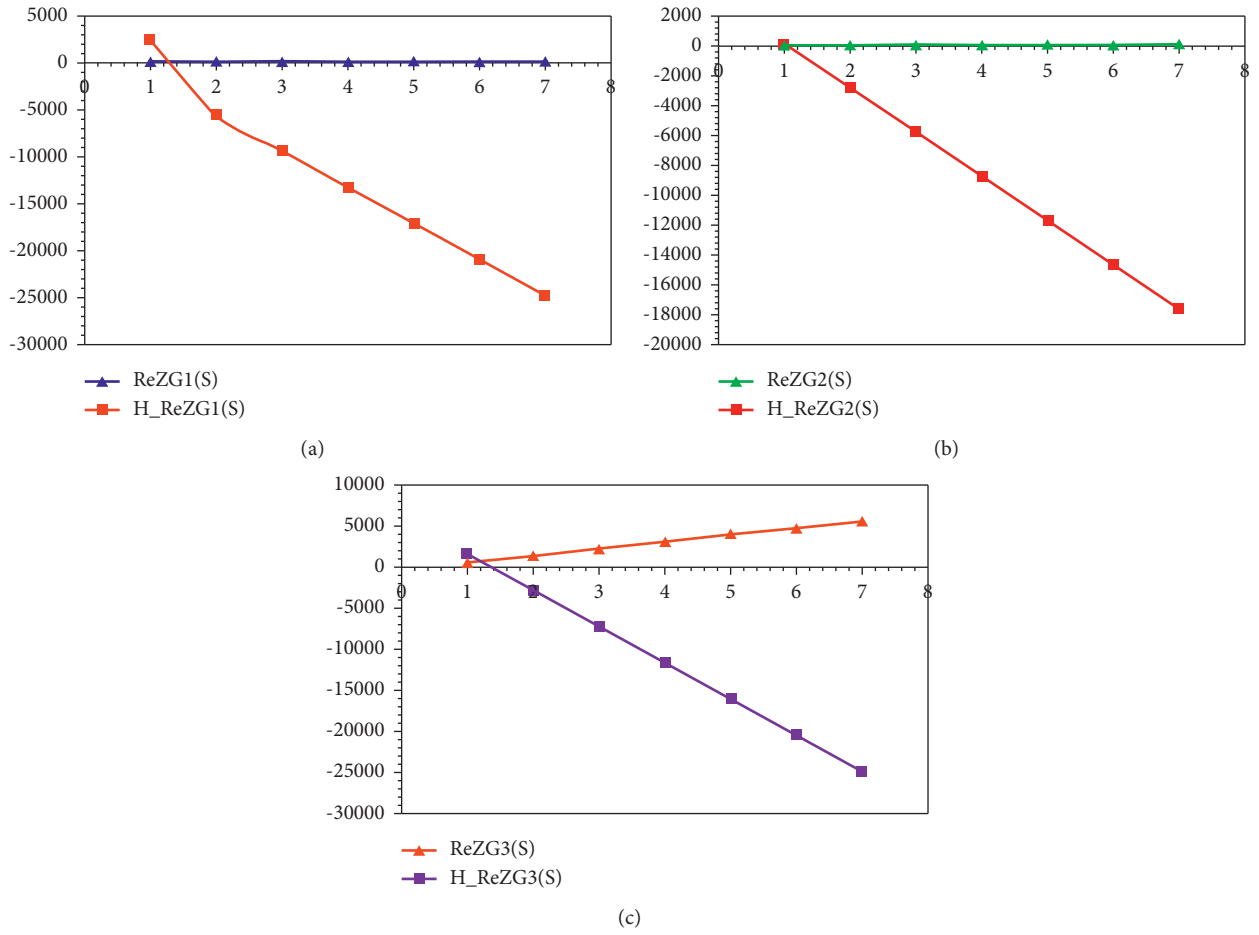

Figure 9: (a) The redefined first Zagreb index, (b) the redefined second Zagreb entropy, and (c) the Redefined third Zagreb index, with respective heat of formation for GST − SL[n].

Numerical results for AZI and J indices are shown in Table 8, while Figure 8 illustrates the results graphically. For the transformation of augmented Zagreb index and Balaban index into the approximate heat of formation of GST − SL[n] at any level can be exercised with the help of the equation as follows:

$$\begin{aligned} H_{AZI} &= 1030 \cdot (-0.014 \cdot AZI + 3.0186), \\ H_J &= 1030 \cdot (-0.1704 \cdot J + 1.6654). \end{aligned} \tag{18}$$

Numerical results of redefined Zagreb indices are shown in Table 9, while Figure 9 illustrates these indices graphically. The transformation of redefined Zagreb entropies into the approximate heat of formation of GST − SL[n] at any cubic level can be employed by using the equation as follows:

$$\begin{aligned} H_{ReG_1}(S) &= 1030 \cdot (-0.412 \cdot ReG_1 + 3.126), \\ H_{ReG_2} &= 1030 \cdot (-0.145 \cdot ReG_2 + 2.321), \\ H_{ReG_3} &= 1030 \cdot (-0.0050 \cdot ReG_3 - 3.2173). \end{aligned} \tag{19}$$

4. Conclusion

In this paper, some degree constructed topological indices are computed which can be used to find out different physicochemical properties. More preciously, we have computed the Randić index, the atom bond connectivity index, the geometric arithmetic index, the first and second Zagreb indices, and the Balaban index. We also determined a relation between the degree constructed topological indices with heat of formation, and then, we discussed the crystal structure of Ge – Sb – Te (GST) and also its applications in different fields. The heat of formation and the entropy measure are computed in this study, which is useful to analyze the thermodynamic properties of the metal-insulator transition. We illustrated the comparison between the degree constructed topological indices and heat of formation, which leads us to know the physicochemical properties of this two-dimensional material GST.

Data Availability

The data used to support the findings of this study are cited at relevant places within the text as references.

Conflicts of Interest

The authors declare that they have no conflicts of interest.

Authors' Contributions

This work was equally contributed by all writers.

References

[1] R. E. Simpson, P. Fons, A. V. Kolobov et al., "Interfacial phase-change memory," *Nature Nanotechnology*, vol. 6, no. 8, pp. 501–505, 2011.

[2] N. Parveen, R. Berni, S. Sudhakaran et al., "Metalloids in plants: a systematic discussion beyond description," *Annals of Applied Biology*, vol. 180, no. 1, pp. 7–25, 2021.

[3] B. Balasubramaniam, N. Singh, P. Kar, A. Tyagi, J. Prakash, and R. K. Gupta, "Engineering of transition metal dichalcogenide-based 2*D* nanomaterials through doping for environmental applications," *Molecular Systems Design & Engineering*, vol. 4, no. 4, pp. 804–827, 2019.

[4] X. B. Li, N. K. Chen, X. P. Wang, and H. B. Sun, "Phase-change superlattice materials toward low power consumption and high density data storage: microscopic picture, working principles, and optimization," *Advanced Functional Materials*, vol. 28, no. 44, pp. 45–55, Article ID 1803380, 2018.

[5] D. P. Wong, M. Aminzare, T.-L. Chou et al., "Origin of band modulation in GeTe-Rich Ge-Sb-Te thin film," *ACS Applied Electronic Materials*, vol. 1, no. 12, pp. 2619–2625, 2019.

[6] J. Feng, A. Lotnyk, H. Bryja et al., "'Stickier'-surface Sb2Te3 templates enable fast memory switching of phase change material GeSb2Te4 with growth-dominated crystallization," *ACS Applied Materials & Interfaces*, vol. 12, no. 29, pp. 33397–33407, 2020.

[7] D. Vukicevic and B. Furtula, "Topological index based on the ratios of geometrical and arithmetical means of end-vertex degrees of edges," *Journal of Mathematical Chemistry*, vol. 46, no. 4, pp. 1369–1376, 2009.

[8] T. Siegrist, P. Jost, H. Volker et al., "Disorder-induced localization in crystalline phase-change materials," *Nature Materials*, vol. 10, no. 3, pp. 202–208, 2011 March.

[9] G. Bianconi, "The entropy of randomized network ensembles," *Europhysics Letters*, vol. 81, no. 2, pp. 28–35, 2008.

[10] N. K. Chen, X. B. Li, X. P. Wang et al., "Metal–insulator transition of Ge–Sb–Te superlattice: an electron counting model study," *IEEE Transactions on Nanotechnology*, vol. 17, no. 1, pp. 140–146, 2017.

[11] Y. M. Chu, M. K. Siddiqui, S. Javed, L. Sherin, and F. Kausar, "On zagreb type molecular descriptors of ceria oxide and their applications," *Journal of Cluster Science*, vol. 11, pp. 1–10, 2021.

[12] D. Bonchev, *Complexity in Chemistry, Introduction and Fundamentals*, Taylor & Francis, Boca Raton, FL, USA, 2003.

[13] S. Manzoor, M. K. Siddiqui, and S. Ahmad, "On entropy measures of molecular graphs using topological indices," *Arabian Journal of Chemistry*, vol. 13, no. 8, pp. 6285–6298, 2020.

[14] A. Balaban, I. Motoc, D. Bonchev, and O. Mekenyan, "Topological indices for structure-activity correlations," *Steric Effects in Drug Design*, Springer, Berlin, Heidelberg, pp. 21–56, 1983.

[15] I. Gutman, B. Ruscic, N. Trinajstić, and C. F. Wilcox Jr, "Graph theory and molecular orbitals. XII. acyclic polyenes," *The Journal of Chemical Physics*, vol. 62, no. 9, pp. 3399–3405, 1975.

[16] I. Gutman and K. C. Das, "The first zagreb index 30 years after," *MATCH Commun. Math. Comput. Chem,* vol. 50, pp. 83–92, 2004.

[17] R. Todeschini and V. Consonni, *Handbook of Molecular Descriptors*, John Wiley & Sons, USA, 2008.

[18] G. H. Shirdel, H. RezaPour, and A. M. Sayadi, "The hyper zagreb index of graph operations," *Iranian Journal of Mathematical Chemistry*, vol. 4, no. 2, pp. 213–220, 2013.

[19] B. Furtula and I. Gutman, "A forgotten topological index," *Journal of Mathematical Chemistry*, vol. 53, no. 4, pp. 1184–1190, 2015.

[20] B. Furtula, A. Graovac, and D. Vukičević, "Augmented zagreb index," *Journal of Mathematical Chemistry*, vol. 48, no. 2, pp. 370–380, 2010.

[21] A. T. Balaban, "Highly discriminating distance-based topological index," *Chemical Physics Letters*, vol. 89, no. 5, pp. 399–404, 1982.

[22] A. T. Balaban and L. V. Quintas, "The smallest graphs, trees, and 4-trees with degenerate topological index," *Journal of Mathematical Chemistry*, vol. 14, pp. 213–233, 1983.

[23] P. S. Ranjini, V. Lokesha, and A. Usha, "Relation between phenylene and hexagonal squeez using harmonic index," *Int J Graph Theory*, vol. 1, pp. 116–121, 2013.

[24] M. K. Siddiqui, M. Naeem, N. A. Rahman, and M. Imran, "Computing topological indicesof certain networks," *Journal of Optoelectronics and Advanced Materials*, vol. 18, no. No. 9-10, pp. 884–892, 2016.

[25] W. Gao and M. R. Farahani, "Degree-based indices computation for special chemical molecular structures using edge dividing method," *Applied Mathematics and Nonlinear Sciences*, vol. 1, no. 1, pp. 94–117, 2015.

[26] W. Gao, M. Siddiqui, M. Naeem, and N. Rehman, "Topological characterization of carbon graphite and crystal cubic carbon structures," *Molecules*, vol. 22, no. 9, pp. 1496–1507, 2017.

[27] M. Imran, M. K. Siddiqui, M. Naeem, and M. A. Iqbal, "On topological properties of symmetric chemical structures," *Symmetry*, vol. 10, no. 173, pp. 1–21, 2018.
[28] M. K. Siddiqui, M. Imran, and A. Ahmad, "On zagreb indices, zagreb polynomials of some nanostar dendrimers," *Applied Mathematics and Computation*, vol. 280, pp. 132–139, 2016.
[29] R. Shayduk and W. Braun, "Epitaxial films for Ge-Sb-Te phase change memory," *Journal of Crystal Growth*, vol. 311, no. 7, pp. 2215–2219, 2009.
[30] A. Lotnyk, U. Ross, T. Dankwort, I. Hilmi, L. Kienle, and B. Rauschenbach, "Atomic structure and dynamic reconfiguration of layered defects in van der waals layered Ge-Sb-Te based materials," *Acta Materialia*, vol. 141, pp. 92–96, 2017.
[31] G. Bulai, O. Pompilian, S. Gurlui et al., "*Ge-Sb-Te* chalcogenide thin films deposited by nanosecond, picosecond, and femtosecond laser ablation," *Nanomaterials*, vol. 9, no. 5, pp. 676–687, 2019.
[32] J.-Y. Lee, J.-H. Kim, D.-J. Jeon, J. Han, and J.-S. Yeo, "Atomic migration induced crystal structure transformation and core-centered phase transition in single crystal Ge2Sb2Te5 nanowires," *Nano Letters*, vol. 16, no. 10, pp. 6078–6085, 2016.
[33] A. Hirata, T. Ichitsubo, P. F. Guan, T. Fujita, and M. W. Chen, "Distortion of local atomic structures in amorphous *Ge-Sb-Te* phase change materials," *Physical Review Letters*, vol. 120, no. 20, pp. 205502–206212, 2018.
[34] M. N. Schneider and O. Oeckler, "Unusual solid solutions in the System Ge-Sb-Te: the crystal structure of 33R-Ge4–xSb2–yTe7(x, y ≈ 0.1) is isostructural to that of Ge3Sb2Te6," *Zeitschrift fur Anorganische und Allgemeine Chemie*, vol. 634, no. 14, pp. 2557–2561, 2008.
[35] U. Ross, A. Lotnyk, E. Thelander, and B. Rauschenbach, "Microstructure evolution in pulsed laser deposited epitaxial Ge-Sb-Te chalcogenide thin films," *Journal of Alloys and Compounds*, vol. 676, pp. 582–590, 2016.